

Effect of Magnetic Field and a Mode-I Crack 3D-Problem in Micropolar Thermoelastic Cubic Medium Possessing Under Three Theories

Kh. Lotfy^{1,2,*}, N. Yahia²

¹Department of Mathematics, Faculty of Science, Zagazig University, Zagazig Egypt, P.O. Box 44519

²Department of Mathematics, Faculty of Science and Arts, Al-mithnab, Qassim University, P.O. Box 931, Buridah 51931, Al-mithnab, Kingdom of Saudi Arabia

Received 13 May 2013; accepted 11 July 2013

ABSTRACT

A model of the equations of two dimensional problems in a half space, whose surface in free of micropolar thermoelastic medium possesses cubic symmetry as a result of a Mode-I Crack is studied. There acts an initial magnetic field parallel to the plane boundary of the half- space. The crack is subjected to prescribed temperature and stress distribution. The formulation in the context of the Lord-Şhulman theory LS includes one relaxation time and Green-Lindsay theory GL with two relaxation times, as well as the classical dynamical coupled theory CD. The normal mode analysis is used to obtain the exact expressions for the displacement, microrotation, stresses and temperature distribution. The variations of the considered variables with the horizontal distance are illustrated graphically. Comparisons are made with the results in the presence of magnetic field. A comparison is also made between the three theories for different depths.

© 2013 IAU, Arak Branch. All rights reserved.

Keywords: GLtheory; Magneto-thermoelasticity; Mode-I Crack; Microrotation; Micropolar thermoelastic medium

1 INTRODUCTION

THE linear theory of elasticity is of paramount importance in the stress analysis of steel, which is the commonest engineering structural material. To a lesser extent, linear elasticity describes the mechanical behavior of the other common solid materials, e.g. concrete, wood and coal. However, the theory does not apply to the behavior of many of the new synthetic materials of the elastomer and polymer type, e.g. polymethyl- methacrylate (Perspex), polyethylene and polyvinyl chloride. The linear theory of micropolar elasticity is adequate to represent the behavior of such materials. For ultrasonic waves i.e. for the case of elastic vibrations characterized by high frequencies and small wavelengths, the influence of the body microstructure becomes significant. This influence of microstructure results in the development of new type of waves, not in the classical theory of elasticity. Metals, polymers, composites, soils, rocks, concrete are typical media with microstructures. More generally, most of the natural and manmade materials including engineering, geological and biological media possess a microstructure. Eringen and Şhubi [1] and Eringen [2] developed the linear theory of micropolar elasticity.

Thermoelasticity theories, which admit a finite speed for thermal signals, have been receiving a lot of attention for the past four decades. In contrast to the conventional coupled thermoelasticity theory based on a parabolic heat equation (Biot, [3]), which predicts an infinite speed for the propagation of heat, these theories involve a hyperbolic

* Corresponding author.

E-mail address: khlotfy_1@yahoo.com, khlotfy_2@yahoo.com (Kh. Lotfy).

heat equation and are referred to as generalized thermoelasticity theories. Two generalizations to the coupled theory were introduced. The first is due to Lord and Shulman [4] who introduced the theory of generalized thermoelasticity with one relaxation time by postulating a new law of heat conduction to replace the classical Fourier's law. Othman [5] constructs the model of generalized thermoelasticity in an isotropic elastic medium under the dependence of the modulus of elasticity on the reference temperature with one relaxation time.

The second generalization to the coupled theory of thermoelasticity is what is known as the theory of thermoelasticity with two relaxation times or the theory of temperature rate dependent thermoelasticity, and was proposed by Green and Lindsay [6]. It is based on a form of the entropy inequality proposed by Green and Laws [7]. Green and Lindsay [6] obtained another version of the constitutive equations. These equations were also obtained independently and more explicitly by Suhubi [8]. This theory contains two constants that act as relaxation times and modifies all the equations of the coupled theory, not only the heat equation. The classical Fourier's law of heat conduction is not violated if the medium under consideration has a center of symmetry. Othman [9] studied the relaxation effects on thermal shock problems in elastic half space of generalized magneto- thermoelastic waves under three theories.

Following various methods, the elastic fields of various loadings, inclusion and inhomogeneity problems, and interaction energy of point defects and dislocation arrangement have been discussed extensively in the past. Generally, all materials have elastic anisotropic properties which mean the mechanical behavior of an engineering material characterized by the direction dependence. The three dimensional study for an anisotropic material is much more complicated to obtain than the isotropic one ,however, due to the large number of elastic constants involved in the calculation. In particular, transversely isotropic and orthotropic materials, which may not be distinguished from each other in plane strain and plane stress, have been more regularly studied. A review of literature on micropolar orthotropic continua shows that Iesan [10], [11], [12] analyzed the static problems of plane micropolar strain of a homogeneous and orthotropic elastic solid, torsion problem of homogeneous and orthotropic cylinders in the linear theory of micropolar elasticity and bending of orthotropic micropolar elastic beams by terminal couple. Nakamura et al. [13] applied the finite element method for orthotropic micropolar elasticity. Recently, Kumar and Choudhary [14], [15], [16], [17], [18] have discussed various problems in orthotropic micropolar continua. Singh and Kumar [19] and Singh [20] have also studied the plane waves in micropolar generalized thermoelastic solid.

Othman and Lotfy [21] studied two-dimensional problem of generalized magneto-thermoelasticity under the effect of temperature dependent properties. Othman and Lotfy [22] studied transient disturbance in a half-space under generalized magneto-thermoelasticity with moving internal heat source. Othman and Lotfy [23] studied the plane waves in generalized thermo-microstretch elastic half-space by using a general model of the equations of generalized thermo-microstretch for a homogeneous isotropic elastic half space. Othman and Lotfy [24] studied the generalized thermo-microstretch elastic medium with temperature dependent properties for different theories. Othman and Lotfy [25-26] studied the effect of magnetic field and inclined load in micropolar thermoelastic medium possessing cubic symmetry under three theories. The normal mode analysis was used to obtain the exact expression for the temperature distribution, thermal stresses, and the displacement components. In the recent years, considerable efforts have been devoted the study of failure and cracks in solids. This is due to the application of the latter generally in industry and particularly in the fabrication of electronic components. Most of the studies of dynamical crack problem are done using the equations of coupled or even uncoupled theories of thermoelasticity [27-30]. This is suitable for most situations where long time effects are sought. However, when short time are important, as in many practical situations, the full system of generalized thermoelastic equations must be used [4].

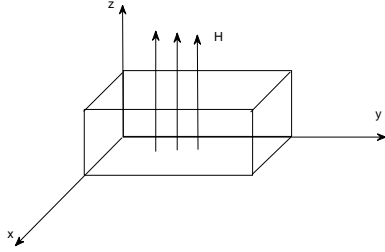
The purpose of the present paper is to determine the normal displacement, normal force stress, and tangential couple stress in a micropolar elastic solid with cubic symmetry. The normal mode analysis used for the problem of generalized thermo-microstretch for an infinite space weakened by a finite linear opening Mode-I crack is solving for the considered variables. The distributions of the considered variables are represented graphically. A comparison is carried out between the temperature, stresses, the couple stress, the microrotation and displacement components as calculated from the generalized thermoelasticity LS, GL and CD theories for the propagation of waves in semi-infinite elastic solids with cubic symmetry.

2 FORMULATION OF THE PROBLEM

We consider a homogeneous, micropolar generalized thermoelastic solid half-space with cubic symmetry. We consider rectangular coordinate system (x, y, z) having origin on the surface $y = 0$ and y -axis pointing vertically into the medium. A magnetic field with constant intensity $H=(0,0,H_0)$ acts parallel to the bounding plane (Table as the

direction of the z -axis). Due to the application of initial magnetic field H , there are results of an induced magnetic field h and an induced electric field E . The simplified linear equations of electrodynamics of slowly moving medium for a homogeneous,

Thermally and electrically conducting elastic solid are,



Geometry of the problem.

$$\text{curl } \mathbf{h} = \mathbf{J} + \epsilon_0 \mathbf{E} \quad (1)$$

$$\text{curl } \mathbf{E} = -\mu_0 \dot{\mathbf{h}} \quad (2)$$

$$\text{div } \mathbf{h} = 0 \quad (3)$$

$$\mathbf{E} = -\mu_0 \left(\dot{\mathbf{u}} \times \mathbf{H} \right) \quad (4)$$

where $\dot{\mathbf{u}}$ is the partial velocity of the medium, and the small effect of temperature gradient on \mathbf{J} is ignored. The dynamic displacement vector is actually measured from a steady state deformed position and the deformation is supposed to be small.

The components of the magnetic intensity vector in the medium are

$$H_x = 0, \quad H_y = 0, \quad H_z = H_0 + h(x, y, z) \quad (5)$$

The electric intensity vector is normal to both the magnetic intensity and the displacement vectors. Thus, it has the components

$$E_x = -\mu_0 H_0 \dot{v}, \quad E_y = \mu_0 H_0 \dot{u}, \quad E_z = 0 \quad (6)$$

The current density vector \mathbf{J} be parallel to \mathbf{E} , thus:

$$J_x = \frac{\partial \mathbf{h}}{\partial y} + \mu_0 H_0 \epsilon_0 \ddot{v}, \quad J_y = -\frac{\partial \mathbf{h}}{\partial x} - \mu_0 H_0 \epsilon_0 \ddot{u}, \quad J_z = 0 \quad (7)$$

$$h = -H_0 (0, 0, e) \quad (8)$$

where e is the dilatation. If we restrict our analysis to plane strain parallel to xy -plane with displacement vector $\mathbf{u} = (u, v, 0)$ and microrotation vector $\boldsymbol{\varphi} = (0, 0, \varphi_3)$ then the field equations and constitutive relations for micropolar thermoelastic solid with cubic symmetry in the absence of body forces. Body couples and heat sources can be written by following the equations given by Minagawa et al., Green Lindsay [6] and Othman and Baljeet as:

$$A_1 \frac{\partial^2 \mathbf{u}}{\partial x^2} + A_3 \frac{\partial^2 \mathbf{u}}{\partial y^2} + (A_2 + A_4) \frac{\partial^2 v}{\partial x \partial y} + (A_3 - A_4) \frac{\partial \varphi_3}{\partial y} + \mu_0 H_0^2 \frac{\partial e}{\partial x} - \mu_0^2 H_0^2 \epsilon_0 \frac{\partial^2 \mathbf{u}}{\partial t^2} - v \frac{\partial}{\partial x} \left(T + t_1 \frac{\partial T}{\partial t} \right) = \rho \frac{\partial^2 \mathbf{u}}{\partial t^2}, \quad (9)$$

$$A_3 \frac{\partial^2 v}{\partial x^2} + A_1 \frac{\partial^2 u}{\partial y^2} + (A_2 + A_4) \frac{\partial^2 u}{\partial x \partial y} - (A_3 - A_4) \frac{\partial \phi_3}{\partial x} + \mu_0 H_0^2 \frac{\partial e}{\partial y} - \mu_0^2 H_0^2 \varepsilon_0 \frac{\partial^2 v}{\partial t^2} - v \frac{\partial}{\partial y} \left(T + t_1 \frac{\partial T}{\partial t} \right) = \rho \frac{\partial^2 v}{\partial t^2}, \tag{10}$$

$$B_3 \nabla^2 \phi_3 + (A_3 - A_4) \left(\frac{\partial v}{\partial x} - \frac{\partial u}{\partial y} \right) - 2(A_3 - A_4) \phi_3 = \rho j \frac{\partial^2 \phi_3}{\partial t^2}, \tag{11}$$

$$K^* \nabla^2 T - \rho C^* (n_1 + t_0 \frac{\partial}{\partial t}) \dot{T} = v T_0 (n_1 + n_0 t_0 \frac{\partial}{\partial t}) \dot{e} \tag{12}$$

$$\sigma_{xx} = A_1 \frac{\partial u}{\partial x} + A_2 \frac{\partial v}{\partial y} - v \left(T + t_1 \frac{\partial T}{\partial t} \right), \tag{13}$$

$$\sigma_{yy} = A_2 \frac{\partial u}{\partial x} + A_1 \frac{\partial v}{\partial y} - v \left(T + t_1 \frac{\partial T}{\partial t} \right), \tag{14}$$

$$\sigma_{xy} = A_4 \left(\frac{\partial u}{\partial y} - \phi_3 \right) + A_3 \left(\frac{\partial v}{\partial x} + \phi_3 \right), \tag{15}$$

$$\sigma_{yx} = A_4 \left(\frac{\partial v}{\partial x} - \phi_3 \right) + A_3 \left(\frac{\partial u}{\partial y} + \phi_3 \right), \tag{16}$$

$$m_{yz} = B_3 \frac{\partial \phi_3}{\partial y}, \tag{17}$$

$$m_{xz} = B_3 \frac{\partial \phi_3}{\partial x}, \tag{18}$$

where σ_{ij} and m_{ij} , are the components of force stress and coupled stress, $v = (A_1 + 2A_2)\alpha_T, \alpha_T$, is coefficient of linear expansion, ρ is the density, j is the microinertia, K^* is the coefficient of thermal conductivity, C^* is the specific heat at constant strain; t_0 and t_1 are the thermal relaxation times, and $\nabla^2 = \frac{\partial^2}{\partial x^2} + \frac{\partial^2}{\partial y^2}$.

For thermoelastic micropolar isotropic medium A_1, A_2, A_3, A_4, B_3 are characteristic constants of the material defined as:

$$A_1 = \lambda + 2\mu + k, \quad A_2 = \lambda, \quad A_3 = \mu + k, \quad A_4 = \mu, \quad B_3 = \gamma \tag{19}$$

For simplification, we shall use the following non- dimensional variables:

$$\bar{x}_i = \frac{\omega^*}{C_0} x_i, \quad \bar{u}_i = \frac{\rho C_0 \omega^*}{v T_0} u_i, \quad \bar{t} = \omega^* t, \quad \bar{t}_0 = \omega^* t_0, \quad \bar{t}_1 = \omega^* t_1, \quad \bar{T} = \frac{T}{T_0}, \quad \bar{\sigma}_{ij} = \frac{\sigma_{ij}}{v T_0}, \tag{20}$$

$$\bar{m}_{ij} = \frac{\omega^*}{C_0 v T_0} m_{ij}, \quad \bar{\phi}_3 = \frac{\rho C_0^2}{v T_0} \phi_3, \quad \bar{g} = \frac{C_0}{\omega^*} g, \quad \{\bar{F}_1, \bar{F}_2\} = \frac{\{F_1, F_2\}}{v T_0}, \quad \bar{h} = \frac{h}{H_0},$$

where $\omega^* = \frac{\rho C^* C_0^2}{K^*}$, $C_0^2 = \frac{A_1}{\rho}$.

Eqs. (9)- (12) take the following form (dropping the dashed for convenience)

$$\alpha \frac{\partial^2 u}{\partial t^2} = \frac{\partial^2 u}{\partial x^2} + \frac{A_3}{A_1} \frac{\partial^2 u}{\partial y^2} + \frac{(A_2 + A_4)}{A_1} \frac{\partial^2 v}{\partial x \partial y} + \frac{(A_3 - A_4)}{A_1} \frac{\partial \phi_3}{\partial y} - R_H \frac{\partial e}{\partial x} - \frac{\partial}{\partial x} \left(T + t_1 \frac{\partial T}{\partial t} \right) \tag{21}$$

$$\alpha \frac{\partial^2 v}{\partial t^2} = \frac{\partial^2 v}{\partial y^2} + \frac{A_3}{A_1} \frac{\partial^2 v}{\partial x^2} + \frac{(A_2 + A_4)}{A_1} \frac{\partial^2 u}{\partial x \partial y} - \frac{(A_3 - A_4)}{A_1} \frac{\partial \phi_3}{\partial x} - R_H \frac{\partial e}{\partial y} - \frac{\partial}{\partial y} \left(T + t_1 \frac{\partial T}{\partial t} \right) \tag{22}$$

$$\nabla^2 \phi_3 + \frac{(A_3 - A_4)C_0^2}{B_3 \omega^{*2}} \left(\frac{\partial v}{\partial x} - \frac{\partial u}{\partial y} \right) - \frac{2(A_3 - A_4)C_0^2}{B_3 \omega^{*2}} \phi_3 = \frac{\rho_j C_0^2}{B_3} \frac{\partial^2 \phi_3}{\partial t^2} \quad (23)$$

$$\nabla^2 T = \left(n_1 + t_0 \frac{\partial}{\partial t} \right) \frac{\partial T}{\partial t} + \varepsilon \left(n_1 + n_0 t_0 \frac{\partial}{\partial t} \right) \frac{\partial}{\partial T} \left(\frac{\partial u}{\partial x} + \frac{\partial v}{\partial y} \right) \quad (24)$$

Introducing potential functions defined by

$$u = \frac{\partial q}{\partial x} + \frac{\partial \psi}{\partial y}, \quad v = \frac{\partial q}{\partial y} - \frac{\partial \psi}{\partial x}, \quad (25)$$

in Eqs. (21) – (24), where $q(x, y, t)$ and $\psi(x, y, t)$ are scalar potential functions, we obtain.

$$\left[\beta^2 \nabla^2 - \alpha \frac{\partial^2}{\partial t^2} \right] q = \left(1 + t_1 \frac{\partial}{\partial t} \right) T \quad (26)$$

$$\left(a_{11} \nabla^2 - \alpha \frac{\partial^2}{\partial t^2} \right) \psi = a_{12} \phi_3 \quad (27)$$

$$a_{13} \nabla^2 \psi + \left(\nabla^2 + 2a_{13} - a_{14} \frac{\partial^2}{\partial t^2} \right) \phi_3 = 0 \quad (28)$$

$$\left[\nabla^2 - \left(n_1 \frac{\partial}{\partial t} + t_0 \frac{\partial^2}{\partial t^2} \right) \right] T = \varepsilon \left(n_1 + n_0 t_0 \frac{\partial}{\partial t} \right) \frac{\partial}{\partial t} \nabla^2 q \quad (29)$$

we can obtain from Eqs. (8) and (25)

$$h = -\nabla^2 q \quad (30)$$

where

$$a_{11} = \frac{A_3}{A_1}, a_{12} = \frac{A_3 - A_4}{A_1}, a_{13} = \frac{(A_4 - A_3)C_0^2}{B_3 \omega^{*2}}, a_{14} = \frac{\rho_j C_0^2}{B_3}, \varepsilon = \frac{v^2 T_0}{\rho \omega^{*2} K}, R_H = \mu_o H_o^2 / \rho C_o^2, \beta^2 = 1 + R_H \quad (31)$$

The solution of the considered physical variables can be decomposed in terms of normal modes as the following form:

$$[\varphi, \psi, e, \sigma_{ij}, q, m_{ij}, T](x, y, t) = [\varphi^*(y), \psi^*(y), e^*(y), \sigma_{ij}^*(y), q^*(y), m_{ij}^*(y), T^*(y)] \exp(\omega t + i a x) \quad (32)$$

where ω is a complex constant and a is the wave number in the x - direction.

Using Eq. (32), Eqs. (26) – (30)

$$(D^2 - a^2 - b^2 \omega^2) q^* - n_3 T^* = 0 \quad (33)$$

$$(D^2 - a^2 - a_1 \omega^2) \psi^* - a_2 \phi_3^* = 0 \quad (34)$$

$$a_{13} (D^2 - a^2) \psi^* + (D^2 - a^2 - 2a_{14} - a_{15} \omega^2) \phi_3^* = 0 \quad (35)$$

$$(D^2 - a^2 - n_4) T^* - \varepsilon^* (D^2 - a^2) q^* = 0 \quad (36)$$

where

$$b^2 = \frac{\alpha}{\beta^2}, \quad a_1 = \frac{\alpha}{a_{11}}, \quad a_2 = \frac{a_{12}}{a_{11}}, \quad n_3 = \frac{1+t_1\omega}{\beta^2}, \quad n_4 = \omega(n_1 + t_0\omega), \quad \varepsilon^* = \varepsilon\omega(n_1 + n_0\omega t_0)$$

Eliminating ψ^*, T^* between Eqs. (36)-(33) we obtain

$$(D^4 - B_1D^2 + B_2)(q^*, T^*) = 0 \tag{37}$$

and

$$\left[D^4 - B_3D^2 + B_4 \right] \{ \varphi^*, \psi^* \} = 0 \tag{38}$$

where

$$B_1 = 2a^2 + n_4 + b^2\omega^2 + n_3\varepsilon^* \tag{39}$$

$$B_2 = a^4 + (n_4 + b^2\omega^2 + n_3\varepsilon^*)a^2 + n_4b^2\omega^2 \tag{40}$$

$$B_3 = 2a^2 + (a_1 + a_{15})\omega^2 - 2a_{13} - a_2a_{13} \tag{41}$$

$$B_4 = a^4 + (a_1\omega^2 - 2a_{13} + a_{14}\omega^2 - a_2a_{13}) + a_1\omega^2(-2a_{13} + a_{14}\omega^2) \tag{42}$$

The solution of Eqs. (37) and (38), which are bounded for $y > 0$, are given by

$$q^* = \sum_{j=1}^2 M_j(a, \omega) e^{-k_j y} \tag{43}$$

$$T^* = \sum_{j=1}^2 M'_j(a, \omega) e^{-k_j y} \tag{44}$$

$$\psi^* = \sum_{n=3}^4 M_n(a, \omega) e^{-k_n y} \tag{45}$$

$$\varphi_3^* = \sum_{n=3}^4 M'_n(a, \omega) e^{-k_n y} \tag{46}$$

where $M_j(a, \omega)$, $M'_j(a, \omega)$, $M_n(a, \omega)$ and $M'_n(a, \omega)$ are some parameters depending on a and ω . k_j^2 , ($j=1,2$) are the roots of the characteristic equation of Eq. (37) and k_n^2 , ($n=3,4$) are the roots of the characteristic equation of Eq. (38).

Using Eqs. (43)- (46) into Eqs. (37) and (38) we get the following relations

$$T^* = \sum_{j=1}^2 R_j M_j(a, \omega) e^{-k_j y} \tag{47}$$

$$\varphi_3^* = \sum_{n=3}^4 R_n M_n(a, \omega) e^{-k_n y} \tag{48}$$

where

$$R_{1,2} = \frac{1}{n_1} [K_{1,2}^2 - a^2 - b^2 \omega^2] \tag{49}$$

$$R_{3,4} = \frac{1}{a_1} [K_{3,4}^2 - a^2 - a_1 \omega^2] \tag{50}$$

The roots $K_{1,2}^2$ and $K_{3,4}^2$ of Eqs. (37) and (38), respectively are given by

$$K_{1,2}^2 = \frac{1}{2} \left(B_1 \pm \sqrt{B_1^2 - 4B_2} \right) \quad (51)$$

$$K_{3,4}^2 = \frac{1}{2} \left(B_3 \pm \sqrt{B_3^2 - 4B_4} \right) \quad (52)$$

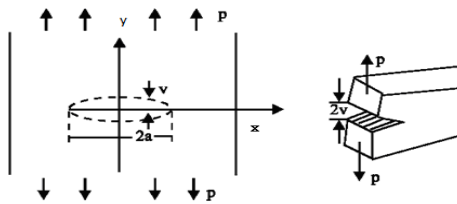
3 APPLICATION

The plane boundary subjects to an instantaneous normal point force and the boundary surface is isothermal, the boundary conditions at the vertical plan $z = 0$ and in the beginning of the crack at $x = 0$ are $\sigma_{yy} = -p(x)$, $|x| < a$

$$T = f(x), \quad |x| < a \quad \text{and} \quad \frac{\partial T}{\partial y} = 0, \quad |x| > a$$

$$\begin{aligned} \sigma_{yx} &= 0, & -\infty < x < \infty \\ m_{yx} &= 0, & -\infty < x < \infty \end{aligned} \quad (53)$$

Using Eq.(20), (25), (26)-(29) on the non-dimensional boundary conditions and using Eq.(43), (45), (47)-(48), we obtain the expressions of displacements, force stress, coupled stress and temperature distribution for micropolar generalized thermoelastic medium with magnetic field as follows:



Displacement of an external mode-i crack.

$$u^*(y) = iaM_1 e^{-k_1 y} + iaM_2 e^{-k_2 y} - k_3 M_3 e^{-k_3 y} - k_4 M_4 e^{-k_4 y} \quad (54)$$

$$v^*(y) = -k_1 M_1 e^{-k_1 y} - k_2 M_2 e^{-k_2 y} - ia(M_3 e^{-k_3 y} + k_4 M_4 e^{-k_4 y}) \quad (55)$$

$$\sigma_{yy}^*(y) = s_1 M_1 e^{-k_1 y} + s_2 M_2 e^{-k_2 y} + s_3 M_3 e^{-k_3 y} + s_4 M_4 e^{-k_4 y} \quad (56)$$

$$\sigma_{yx}^*(y) = r_1 M_1 e^{-k_1 y} + r_2 M_2 e^{-k_2 y} + r_3 M_3 e^{-k_3 y} + r_4 M_4 e^{-k_4 y} \quad (57)$$

$$m_{yz}^*(y) = -B_3(k_3 R_3 M_3 e^{-k_3 y} + k_4 R_4 M_4 e^{-k_4 y}) w^{*2} / \rho C_o^4 \quad (58)$$

$$T^*(y) = R_1 M_1 e^{-k_1 y} + R_2 M_2 e^{-k_2 y} \quad (59)$$

where

$$\begin{aligned} s_1 &= (-a^2 A_2 / \rho C_o^2 + A_1 k_1^2 / \rho C_o^2 - R_1(1 + wt_1)), \quad s_2 = (-a^2 A_2 / \rho C_o^2 + A_1 k_2^2 / \rho C_o^2 - R_2(1 + wt_1)) \\ s_3 &= iak_3(A_1 - A_2) / \rho C_o, \quad s_4 = iak_4(A_1 - A_2) / \rho C_o^2, \\ r_1 &= -iak_1(A_3 + A_4) / \rho C_o^2, \quad r_2 = -iak_2(A_3 + A_4) / \rho C_o^2, \\ r_3 &= (a^2 A_4 + R_3(A_3 - A_4) + A_3 k_3^2) / \rho C_o^2, \quad r_4 = (a^2 A_4 + R_4(A_3 - A_4) + A_3 k_4^2) / \rho C_o^2. \end{aligned} \quad (60)$$

Invoking the boundary conditions (53) at the surface $y=0$ of the plate, we obtain a system of four equations. After applying the inverse of matrix method, we have the values of the four constants $M_j, j=1,2$, and $M_n, n=3,4$. Hence, we obtain the expressions of displacements, force stress, coupled stress and temperature distribution for micropolar generalized thermoelastic medium.

4 NUMERICAL RESULTS AND DISCUSSIONS

In order to illustrate the theoretical results obtained in preceding section and to compare these in the context of various theories of thermoelasticity, we now present some numerical results. In the calculation process, we take the case of magnesium crystal (Eringen) as material subjected to mechanical and thermal disturbances for numerical calculations considering the material medium as that of copper. Since, ω is complex, then we take $\omega = \omega_0 + i\zeta$. The other constants of the problem are taken as $\omega_0 = -2, \zeta = 1$, The physical constants used are: $p = 1, f = 1$

$$\begin{aligned} \rho &= 1.74 \text{ gm/cm}^3, \quad j = 0.2 \times 10^{-15} \text{ cm}^3, \quad \lambda = 9.4 \times 10^{11} \text{ dyne/cm}^2, \quad T_0 = 23 \text{ }^\circ\text{C}, \\ \mu &= 4.0 \times 10^{11} \text{ dyne/cm}^2, \quad K = 1.0 \times 10^{11} \text{ dyne/cm}^2, \quad \gamma = 0.779 \times 10^{-4} \text{ dyne}, \\ K^* &= 0.6 \times 10^{-2} \text{ cal/cm sec }^\circ\text{C}, \quad C^* = 0.23 \text{ cal/gm }^\circ\text{C}. \quad a = 2, \quad t = 0.1 \end{aligned}$$

The results are shown in Figs. 1-6. The graph shows the three curves predicted by different theories of thermoelasticity. In these Figures, the solid lines represent the solution in the Coupled theory, the dotted lines represent the solution in the generalized Lord and Shulman theory and dashed lines represent the solution derived using the Green and Lindsay theory. These Figures represent the solution obtained using the coupled theory (CD theory: $n_0 = 0, n_1 = 1, n_2 = 1, t_0 = 0, t_1 = 0$), the generalized theory with one relaxation time (Lord-Shulman theory LS theory: $n_0 = 1, n_1 = 1, n_2 = 1, t_0 = 0.02, t_1 = 0$), and generalized theory with two relaxation times (Green-Lindsay theory (GL theory: $n_0 = 0, n_1 = 1, n_2 = 1, t_0 = 0.02, t_1 = 0.03$)).

We notice that the results for the temperature, the displacement and stresses distribution when the relaxation time is including in the heat equation are distinctly different from those when the relaxation time is not mentioned in heat equation, because the thermal waves in the Fourier's theory of heat equation travel with an infinite speed of propagation as opposed to finite speed in the non-Fourier case. This demonstrates clearly the difference between the coupled and the generalized theories of thermoelasticity. Figs. 1-6. The graph shows the two cases when the magnetic field acts on the material and when absence, from this Figures., we obtain the effect of magnetic field caused rearranged the atoms in the medium and compact the curves. For the value of y , namely $y = 0.2$, were substituted in performing the computation. It should be noted (Fig.1) that in this problem, the crack's size, x is taken to be the length in this problem so that $0 \leq x \leq 1$ (when H_0 exist) and $0 \leq x \leq 2$ (when $H_0 = 0.0$), $y = 0$ represents the plane of the crack that is symmetric with respect to the y plan. It is clear from the graph that T has maximum value at the beginning of the crack ($x = 0$), it begins to fall just near the crack edge ($x = 1$), where it experiences sharp decreases (with maximum negative gradient at the crack's end). The value of temperature quantity converges to zero with increasing the distance x .

Fig. 2, the horizontal displacement, u , begins with increase then smooth decreases again to reach its maximum magnitude just at the crack end. Beyond it u falls again to try to retain zero at infinity. Fig. 3, the vertical displacement v , we see that the displacement component v always starts from the negative value and terminates at the zero value. Also, at the crack end to reach minimum value, beyond reaching zero at the double of the crack size (state of particles equilibrium). The displacements u and v show different behaviours, because of the elasticity of the solid tends to resist vertical displacements in the problem under investigation. Both of the components show different behaviours, the former tends to increase to maximum just before the end of the crack. Then it falls to a minimum with a highly negative gradient. Afterwards it rises again to a maximum beyond about the crack end.

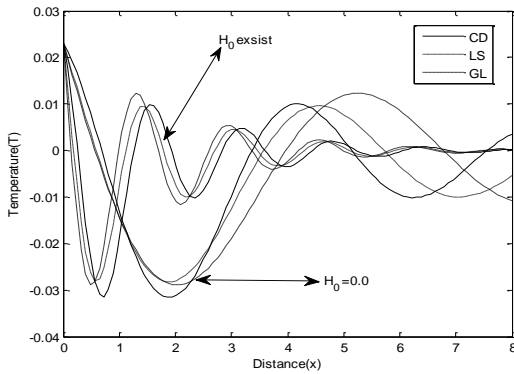


Fig. 1
Variation of temperature distribution T with different theories.

The stress component, σ_{xx} reach coincidence with negative value (Fig.4) and satisfy the boundary condition at $x = 0$, reach the maximum value near the end of crack ($x \approx 1$) and converges to zero with increasing the distance x . Fig. 5, shows that the stress component σ_{yy} satisfy the boundary condition at $X = 0$ and had a different behaviour. It decreases in the start and start decreases (maximum) in the context of the three theories until reaching the crack end ($x \approx 1$). These trends obey elastic and thermoelastic properties of the solid under investigation. Fig.6, the tangential coupled stress m_{xy} satisfies the boundary condition at $X = 0$. It decreases in the start and start increases (maximum) in the context of the three theories then smooth decreasing until reaching the crack end. The effect of the magnetic field down load the magnitude of the front of wave propagation.

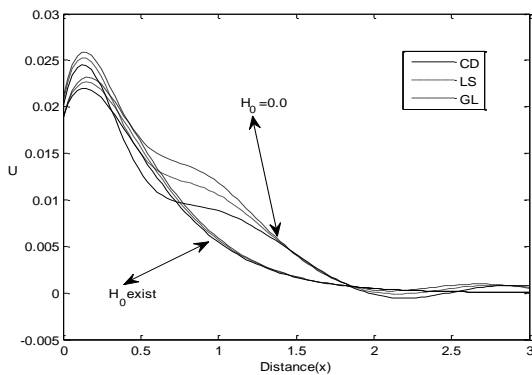


Fig. 2
Variation of displacement distribution u with different theories.

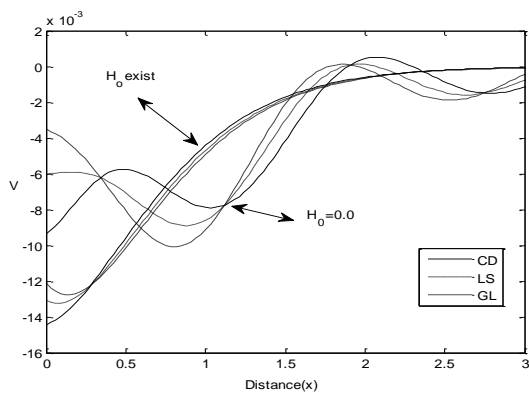


Fig. 3
Variation of displacement distribution v with different theories.

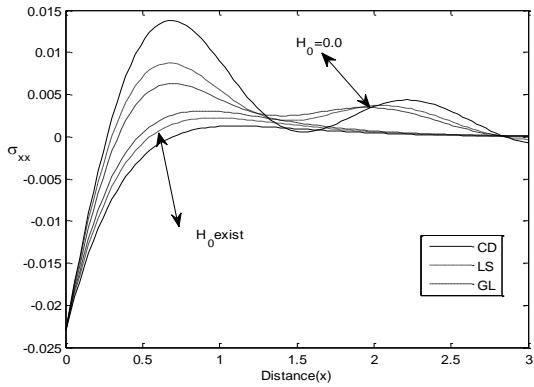


Fig. 4
Variation of stress distribution σ_{yy} with different theories.

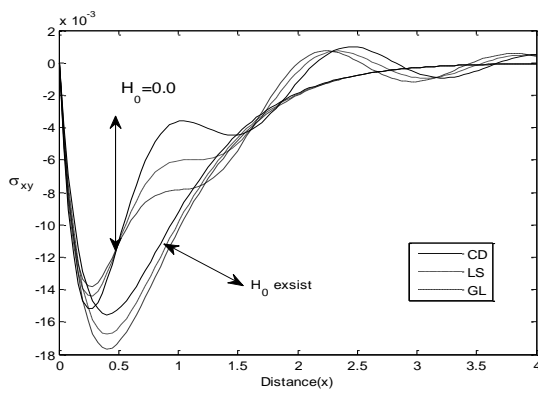


Fig. 5
Variation of stress distribution σ_{yx} at with different theories.

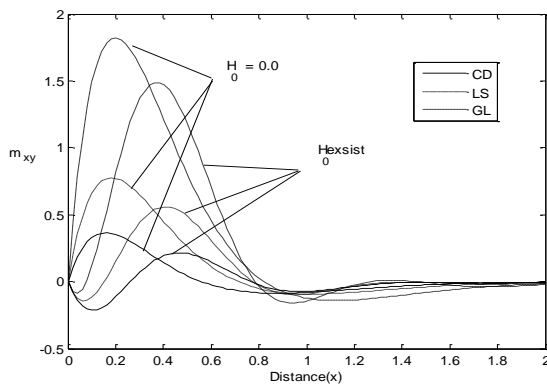


Fig. 6
Variation of tangential couple stress m_{xy} with different theories.

Fig. 7-15 show the comparison between the temperature T , displacement components u, V , the force stresses components σ_{xx}, σ_{xy} , and the tangential coupled stress m_{xy} , the case of different three values of y , (namely $y=0.1, y=0.2$ and $y=0.3$) under GL theory. It should be noted (Fig.7) that in this problem. It is clear from the graph that T has maximum value at the beginning of the crack ($x=0$), it begins to fall just near the crack edge ($x=1$), where it experiences sharp decreases (with maximum negative gradient at the crack's end). Graph lines for both values of y show different slopes at crack ends according to y -values. In other words, the temperature line for $y=0.1$ has the highest gradient when compared with that of $z=0.2$ and $z=0.3$ at the first of the range. In addition, all lines begin to

coincide when the horizontal distance x is beyond the double of the crack size to reach the reference temperature of the solid. These results obey physical reality for the behaviour of copper as a polycrystalline solid, it shown also in Fig: 8.

Fig. 9, the horizontal displacement u , despite the peaks (for different vertical distances $y=0.1, y=0.2$ and $y=0.3$) occur at equal value of x , the magnitude of the maximum displacement peak strongly depends on the vertical distance y . It is also clear that the rate of change of u decreases with increasing y as we go farther apart from the crack Fig. 10. On the other hand, Fig. 11 shows atonable increase of the vertical displacement, v , near the crack end to reach maximum value beyond $x = 1$ reaching zero at the double of the crack size (state of particles equilibrium). Fig.12, the vertical stresses σ_{xx} Graph lines for both values of y show different slopes at crack ends according to y -values. In other words, the σ_{xx} component line for $y = 0.1$ has the lowest gradient when compared with that of $y = 0.2$ and $y= 0.3$ at the edge of the crack. In addition, all lines begin to coincide when the horizontal distance x is beyond the double of the crack size to reach zero after their relaxations at infinity. Variation of y has a serious effect on both magnitudes of mechanical stresses. These trends obey elastic and thermoelastic properties of the solid under investigation.

Fig. 13, shows that the stress component σ_{xy} satisfy the boundary condition, the line for $z = 0.3$ has the highest gradient when compared with that of $z = 0.2$ and $z= 0.1$ and converge to zero when $x > 3$. These trends obey elastic and thermoelastic properties of the solid, it is shown also in Fig. 14. Fig. 15, the tangential coupled stress m_{xy} it increases in the start and start decreases in the context of the three values of y until reaching the crack end, for $y = 0.1$ has the highest gradient when compared with that of $z = 0.2$ and $z= 0.3$ at the edge of the crack. All lines begin to coincide when the horizontal distance x is beyond the edge of the crack.

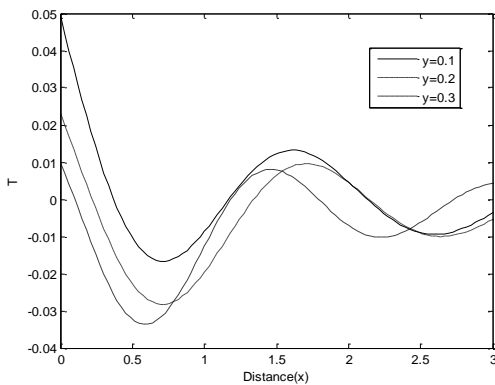


Fig. 7
Temperature distribution T with variation of distances under GL theory.

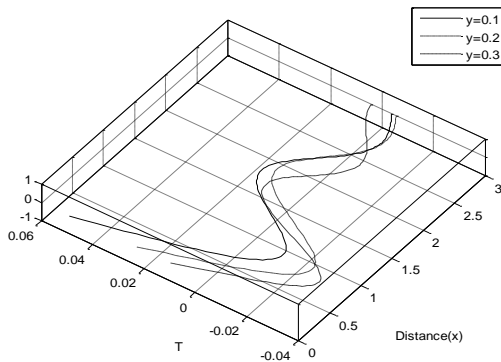


Fig. 8
Temperature distribution T with variation of distances under GL theory in 3D.

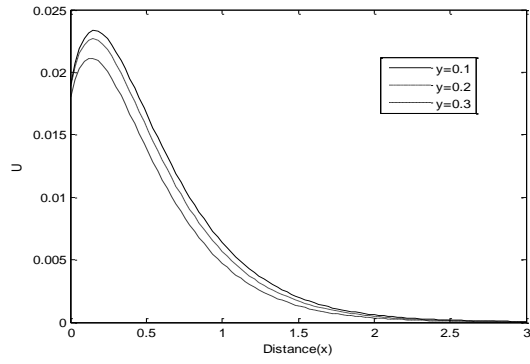


Fig. 9
Displacement distribution u with variation of distance under GL theory.

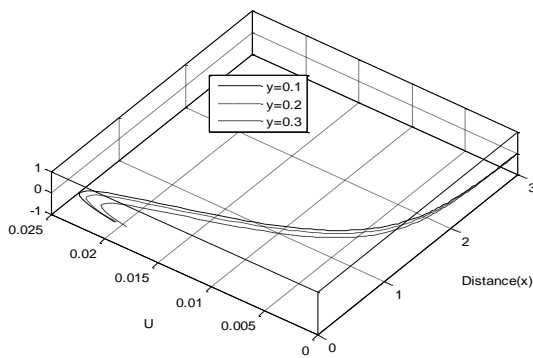


Fig. 10
Displacement distribution u with variation of distance under GL theory in (3D).

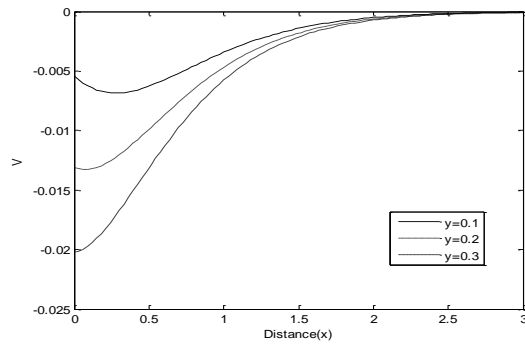


Fig. 11
Displacement distribution v with variation of distance under GL theory.

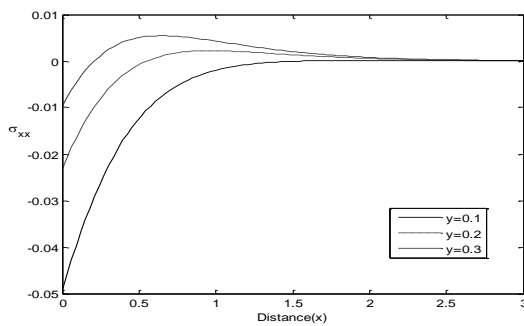
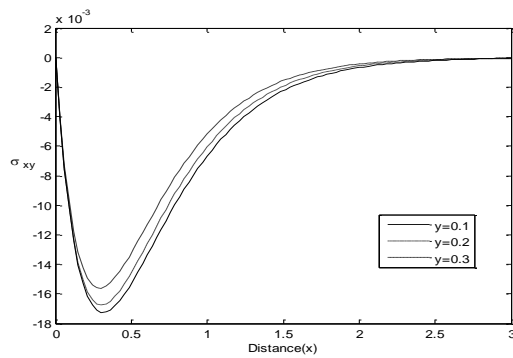
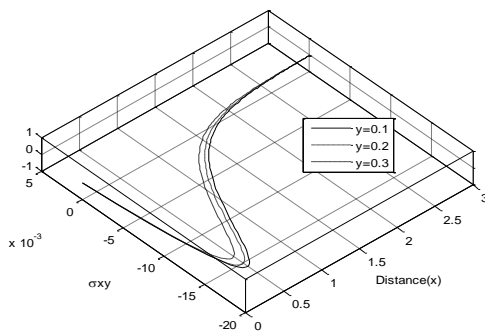


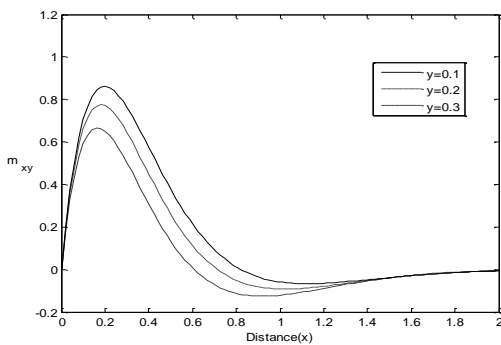
Fig. 12
Stress distribution σ_{xx} with variation of distance under GL theory.

**Fig. 13**

Stress distribution σ_{xy} with variation of distance under GL theory.

**Fig. 14**

Stress distribution σ_{xy} with variation of distance under GL theory.

**Fig. 15**

Tangential couple stress m_{xy} with variation of distance under GL theory.

Finally The Figs. 16-21 shows the 3D plots for the physical components under Lord-Şhulman theory with the effect of magnetic field. Fig. 16 Shows the variation of the temperature and the depth with increasing x under the effects of magnetic field, which it decreases with increasing of wave speed until approaching to zero, as well it decreases with decreasing of the value of depth. Fig. 17 Shows the variation of two horizontal displacement u and the depth with increasing x under the effects of magnetic field. The value of the displacement u components has an oscillatory behavior with magnetic field in the whole range of the magnetic field. Fig. 18 Shows the variation vertical displacement v and the depth with increasing x (when the waves translate from a side to another through the crack (as two layers)) waves under the effects of magnetic field. The effect of magnetic on vertical displacement v wave which it decreases and increases periodically, as well it decreases with increasing of the value of wave speed. Fig. 19 Show the variation of normal stress σ_{yy} in 3D under the effect of magnetic field. The effect of magnetic field on normal stress which it oscillatory behavior with increasing of magnetic field, as well it decreases with

increasing of the value of wave speed. Fig. 20 Show the variation of stress component σ_{xy} . The value of the stress component σ_{xy} has an oscillatory behavior with magnetic field in the whole range of the phase velocity. Fig. 21, the tangential coupled stress m_{xy} in 3D, it increases in the start and start decreases in the context of the three values of y until reaching the crack end,

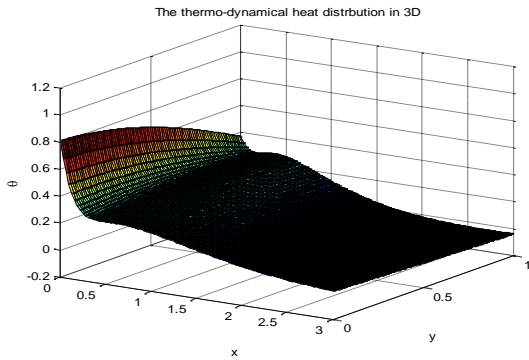


Fig. 16
Temperature distribution T with variation of distances under GL theory and magnetic field.

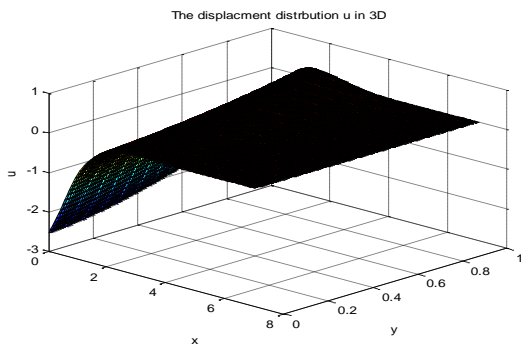


Fig. 17
3D displacement component u with variation of distances under GL theory and magnetic field.

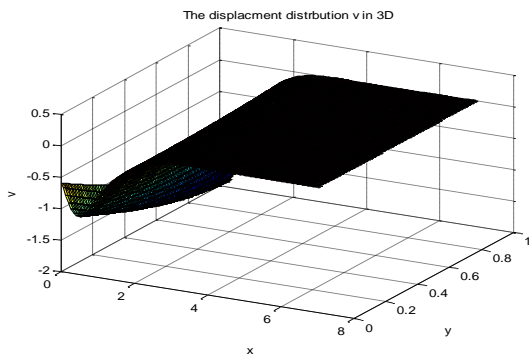


Fig. 18
3D displacement component v with variation of distances under GL theory and magnetic field.

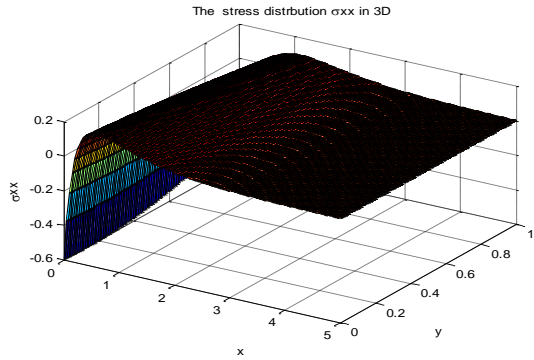


Fig. 19
3D normal stress component with variation of distances under GL theory and magnetic field.

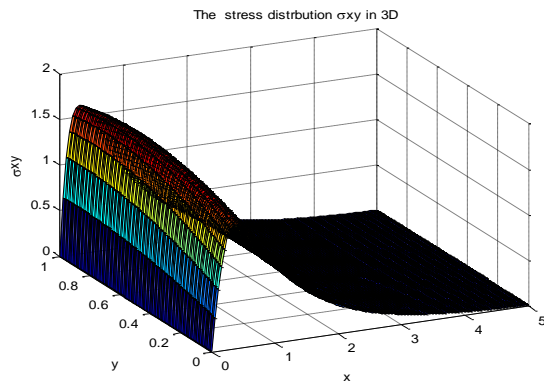


Fig. 20
3D shear stress component with variation of distances under GL theory and magnetic field.

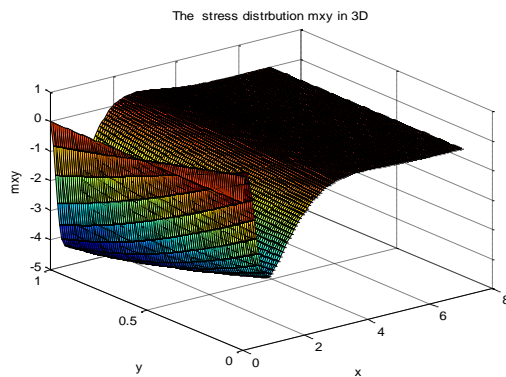


Fig. 21
3D tangential couple stress m_{xy} with variation of distances under GL theory and magnetic field.

7 CONCLUSIONS

Due to the complicated nature of the governing equations of the elasticity-electromagnetic theory, the work done in this field is unfortunately limited in number. The method used in this study provides a quite successful in dealing with such problems. This method gives exact solutions in the elastic medium without any assumed restrictions on the actual physical quantities that appear in the governing equations of the problem considered. Important phenomena are observed in all these computations:

1. The curves in the context of the (CD), (L-S) and (G-L) theories decrease or increasing exponentially with increasing x , this indicate that the thermoelastic waves are unattenuated and nondispersive, where purely thermoelastic waves undergo both attenuation and dispersion.

2. The presence of magnetic field plays a significant role in all the physical quantities.
3. The curves of the physical quantities with (G-L) theory in most of figures are greater in comparison with those under (CD and (L-S) theories.
4. Analytical solutions based upon normal mode analysis for thermoelastic problem in solids have been developed and utilized.
5. A linear opening mode-I crack has been investigated and studied for copper solid.
6. Temperature, radial and axial distributions were estimated at different distances from the crack edge.
7. The stresses distributions, the tangential coupled stress and the values of microstress were evaluated as functions of the distance from the crack edge.
8. Crack dimensions are significant to elucidate the mechanical structure of the solid.
9. Cracks are stationary and external stress is demanded to propagate such cracks.
10. It can be concluded that a change of volume is attended by a change of the temperature while the effect of the deformation upon the temperature distribution is the subject of the theory of thermoelasticity.
11. The value of all the physical quantities converges to zero with an increase in distance x and all functions are continuous.
12. Deformation of a body depends on the nature of forced applied as well as the type of boundary conditions.
13. It is clear from all the figures that all the distributions considered have a non-zero value only in a bounded region of the half-space. Outside of this region, the values vanish identically and this means that the region has not felt thermal disturbance yet.
14. The results presented in this paper should prove useful for researchers in material science, designers of new materials.
15. Study of the phenomenon of relaxation time and magnetic is also used to improve the conditions of oil extractions.

REFERENCES

- [1] Eringen A. C., Suhubi E. S., 1964, Nonlinear theory of simple micropolar solids, *International Journal of Engineering Science* **2**:1-18.
- [2] Eringen A. C., 1966, Linear theory of micropolar elasticity, *Journal of Applied Mathematics and Mechanics* **15**: 909-924.
- [3] Biot M. A., 1956, Thermoelasticity and irreversible thermodynamics, *Journal of Applied Physics* **27**:240-253.
- [4] Lord H. W., Shulman Y., 1967, A generalized dynamical theory of thermoelasticity, *Journal of the Mechanics and Physics of Solids* **15**:299-306.
- [5] Othman M. I. A., 2002, Lord-shulman theory under the dependence of the modulus of elasticity on the reference temperature in two-dimensional generalized thermo- elasticity, *Journal of Thermal Stresses* **25**:1027-1045.
- [6] Green A. E., Lindsay K.A., 1972, Thermoelasticity, *Journal of Elasticity* **2**:1-7.
- [7] Green A. E., Laws N., 1972, On the entropy production inequality, *Archive for Rational Mechanics and Analysis* **45**:47-53.
- [8] Suhubi E. S., 1975, *Thermoelastic Solids in Continuum Physics*, Part 2, Chapter2, Academic Press, New York.
- [9] Othman M. I. A., 2004, Relaxation effects on thermal shock problems in an elastic half-space of generalized magneto-thermoelastic waves, *Mechanics and Mechanical Engineering* **7**:165-178.
- [10] Iesan D., 1973, The plane micropolar strain of orthotropic elastic solids, *Archives of Mechanics* **25**:547-561.
- [11] Iesan D., 1974, Torsion of anisotropic elastic cylinders, *Journal of Applied Mathematics and Mechanics* **54**:773-779.
- [12] Iesan D., 1974, *Bending of Orthotropic Micropolar Elastic Beams by Terminal Couples*, An State University Lasi **20**: 411- 418.
- [13] Nakamura S., Benedict R., Lakes R., 1984, Finite element method for orthotropic micropolar elasticity, *International Journal of Engineering Science* **22**:319-330.
- [14] Kumar R., Choudhary S., 2002, Influence and green's function for orthotropic micropolar continua, *Archives of Mechanics* **54**:185-198.
- [15] Kumar R., Choudhary S., 2002, Dynamical behavior of orthotropic micropolar elastic medium, *Journal of vibration and control* **5**:1053- 1069.
- [16] Kumar R., Choudhary S., 2002, Mechanical sources in orthotropic micropolar continua, *Proceedings of the Indian Academy of Sciences* **111**(2):133-141.
- [17] Kumar R., Choudhary S., 2003, Response of orthotropic micropolar elastic medium due to various sources, *Meccanica* **38**:349- 368.
- [18] Kumar R., Choudhary S., 2004, Response of orthotropic micropolar elastic medium due to time harmonic sources, *Sadhana* **29**:83- 92.

- [19] Singh B., Kumar R., 1998, Reflection of plane wave from a flat boundary of micropolar generalized thermoelastic half-space, *International Journal of Engineering Science* **36**:865-890.
- [20] Singh B., 2000, Reflection of plane sound wave from a micropolar generalized thermoelastic solid half-space, *Journal of sound and vibration* **235**:685-696.
- [21] Othman M.I. A., Lotfy KH., 2009, Two-dimensional Problem of generalized magneto-thermoelasticity under the Effect of temperature dependent properties for different theories, *Multidiscipline Modeling in Materials and Structures* **5**:235-242.
- [22] Othman M.I. A., Lotfy KH., Farouk R.M., 2009, Transient disturbance in a half-space under generalized magneto-thermoelasticity due to moving internal heat source, *Acta Physica Polonica A* **116**:186-192.
- [23] Othman M.I. A., Lotfy KH., 2010, On the plane waves in generalized thermo-microstretch elastic half-space, *International Communication in Heat and Mass Transfer* **37**:192-200.
- [24] Othman M.I. A., Lotfy KH., 2009, Effect of magnetic field and inclined load in micropolar thermoelastic medium possessing cubic symmetry, *International Journal of Industrial Mathematics* **1**(2): 87-104.
- [25] Othman M.I. A., Lotfy KH., 2010, Generalized thermo-microstretch elastic medium with temperature dependent properties for different theories, *Engineering Analysis with Boundary Elements* **34**:229-237.
- [26] Lotfy Kh., 2014, Two temperature generalized magneto-thermoelastic interactions in an elastic medium under three theories, *Applied Mathematics and Computation* **227**:871-888.
- [27] Dhaliwal R., 1980, External Crack due to Thermal Effects in an Infinite Elastic Solid with a Cylindrical Inclusion, *Thermal Stresses in Server Environments*, Doi: 10.1007/978-1-4613-3156-8_41.
- [28] Hasanyan D., Librescu L., Qin Z., Young R., 2005, Thermoelastic cracked plates carrying nonstationary electrical current, *Journal of Thermal Stresses* **28**:729-745.
- [29] Ueda S., 2003, Thermally induced fracture of a piezoelectric Laminate with a crack normal to interfaces, *Journal of Thermal Stresses* **26**:311-323.
- [30] Elfalaky A., Abdel-Halim A. A., 2006, A mode-i crack problem for an infinite space in thermoelasticity, *Journal of Applied Sciences* **6**:598-606.